NUMERICAL INVESTIGATION OF COUNTER-ROTATING VORTICAL GUST IMPINGEMENT EFFECT ON A ROTATING CYLINDER

UDC: 621.643:621.1.016
Original scientific paper https://doi.org/10.18485/aeletters.2019.4.1.2

Muhammad Arsalan Anwar[1], Shehryar Manzoor[1]

[1]Mechanical Engineering Department, University of Engineering and Technology, Taxila, Pakistan

Abstract:
The influence of a counter-rotating vortical gust pair is numerically investigated on a streamlined laminar flow and forced convection heat transfer around a steadily rotating two-dimensional circular cylinder. Reynolds number is kept to a fixed value of 100 based on cylinder diameter (D). The working fluid used is water having a fixed Prandtl number of 7. The non-dimensional rotation rate is altered within the vortex shedding regime i.e. $0 \leq \alpha \leq 1.5$ in the steps of 0.25. The numerical results were computed via commercially accessible CFD software package FLUENT®. The governing flow equations are continuity, momentum, and energy equations have been resolved via constant wall temperature (CWT) boundary condition. The numerical outcomes are computed illustrating the variation in the lift coefficient, Strouhal number, average and local Nusselt number, vorticity and temperature contours around the isothermal rotating cylinder. The influence of the vortical gust is observed to stretch the shear layer in a typical manner. The vortical gust can be treated as an additional heat transfer suppression technique in conjunction with rotation for a circular cylinder.

ARTICLE HISTORY
Received: 27.03.2019.
Accepted: 29.03.2019.
Available: 31.03.2019.

KEYWORDS
vortical gust, laminar flow, vortex shedding regime, rotating cylinder, heat transfer suppression

1. INTRODUCTION

Flow past a circular cylinder has become a unique scenario in fluid dynamics and from heat transfer perspectives during the past decades. The type of flow involves many useful applications regarding the design of offshore platforms, masts, tubes in heat exchangers, textile, food processing, flow control devices, chemical-reaction towers, aerodynamic and marine industry.

Fornberg [1] studied the viscous flow around a circular cylinder in the steady regime for a Reynolds number up to 300 by employing a unique technique centered on Newton's method. Lange et al. [2]studied the flow behaviour effect at low Reynolds number range ($0 \leq Re \leq 45.9$) on a cylinder. The flow remains steady and two regular symmetrical vortices enlarge behind the cylinder surface whereas, a vortex shedding occurs by augmenting the Re by means of a vortex detachment as proposed by Badr et al. [3]. Barkley and Henderson [4] predicted the flow transition for a fixed cylinder at Re = 47 from steady to 2-D periodic and finally to 3-D periodic for Re = 188.5 respectively. On the other hand, Williamson [5] revealed the periodic 3-D transition of the flow at Re = 194. The similar phenomenon was analyzed by Baranyi [6] at Re = 160 for a circular cylinder.

Roshko [7] performed experiments on a rotating cylinder for higher Reynolds number range (10^6 to 10^7) and analyzed the vortex shedding occurrence for Reynolds number higher than 3.5×10^6. Coutanceau and Menard [8] examined an immediate wake formation behind an impulsively commenced circular cylinder under an influence of different rotation rates via flow visualization technique. The rotation causes much earlier

CONTACT: M. Arsalan Anwar, e-mail: arsalan116c@gmail.com

detachment of positive and negative vortices in comparison to a still cylinder case. Ingham and Tang [9] performed the numerical solutions for a rotating circular cylinder by a unique numerical technique at Reynolds number of 5 and 20 for a certain range of rotation rate ($0 \leq \alpha \leq 3$). The computed results are in a good promise with the findings made by Badr and Dennis [10]. Later on, Kang et al. [11] investigated the laminar two-dimensional flow past a spinning circular cylinder at a fixed Re of 60, 100 and 160 for specified rotation rates ($0 \leq \alpha \leq 2.5$). The shedding of positive and negative vortices occurs at low rotational rates and entirely suppressed at critical rotational rates that directly resembles a logarithmic reliance on Reynolds number. Hieber and Gebhart [12] studied the heat transfer via forced convection around a circular cylinder at small values of Reynolds number by employing the technique of matched asymptotic expansion. Kendoush [13] approximated an analytical solution via relevant velocity components in an energy equation to propose an average Nusselt number relationship for a spinning cylinder at a fixed temperature to observe the transfer of heat by forced convection. Mahfouz and Badr [14] stated an increase in heat transfer rate in the lock-in region from a rotationally oscillating cylinder for Re between 40 and 200. Stojković et al. [15] studied the distinct higher rotation rates impact on a circular cylinder corresponding to steady as well as unsteady laminar flow regime. The vortex shedding was observed to completely disappear at α = 1.8 in an unsteady regime. Mittal and Kumar [16] examined the 2-D flow encircling a spinning circular cylinder at fixed Reynolds number of 200 for rotation rates between 0 and 5 ($0 \leq \alpha \leq 5$). The vortex shedding was diminished comprehensively at a spinning rate less than equal to 1.91($\alpha \leq 1.91$) and the formation of asymmetric vortices was observed for the second vortex shedding regime.

In contrast, Sanitjai and Goldstein [17] analyzed the heat transfer phenomenon round a circular cylinder between the Prandtl number (Pr) of 0.7 and 176 for higher Re values in the forced convection mode. Heat transfer rate firmly influenced by the Re and the diverse power indices range intended for a Prandtl number. Ishak et al. [18] determined the rate of heat transfer around a circular cylinder via an unsteady mixed convection boundary layer flow close to a vertical stretching sheet. An enhancement in the Nusselt number was observed in a direct correspondence with the Prandtl number. Bharti et al. [19] performed numerical simulations for an unconfined circular cylinder between Re of 10 to 45 and the Pr ranges from 0.7 to 400. The reported results suggested a rise in Nusselt number on a surface at a fixed point with an increase in Re and Pr. Paramane and Sharma [20] depicted the heat transfer suppression for a circular cylinder that turns out to be independent of Reynolds number as well as applied thermal boundary conditions at higher rotation rates via finite volume framework. Patnana et al. [21] numerically described the average Nusselt number augmentation in conjunction with Re and Pr for power-law fluids corresponding to several power-law index values between Re of 40 and 180. Sarkar et al. [22] reported the results in a periodic laminar flow regime for Re varies from 80 and 180 in order to determine the heat transfer rate for a cylinder under the impact of Prandtl number and for a certain range of Richardson number ($0 \leq Ri \leq 3$). It was shown that the Nusselt number enhanced with Prandtl number and an opposite trend was analyzed for the Ri raised from zero to unity. In contrast, average Nusselt number reduces at higher rotation rates for particular values of Re and Pr in a steady flow regime as proposed by Sharma and Dhiman [23]. Sufyan et al. [24] explored the suppression of heat transfer for a rotating cylinder at higher Pr values, even at inferior spinning rates. The influence of a single gust impulse on a rotating circular cylinder has been studied by Ikhtiar et al. [25], revealed the interesting facts regarding the Nusselt number behaviour. Heat transfer rate decreases in the first and second vortex shedding regimes whereas an opposite phenomenon was observed in an intermediate vortex suppression zone. Later on, Rana et al. [26] presented the results for a rotating cylinder conforming seven distinct gust profiles imparted to a mean flow for a vortex suppression regime. The gust causes a vortex detachment along with an asymmetric formation of vortical structures in the flow stream for a representative vortex suppression regime.

In this research, the effect of a single counter-rotating vortical gust pair has been studied on a rotating circular cylinder in a vortex shedding regime in terms of flow and heat transfer characteristics. The vortical gust pair is introduced by means of a suitable technique, probably for the first time and corresponds to the novelty of a defined problem. The circular cylinder is chosen as the analysis target. Desired outcomes based on the assessment for an Average and Local Nusselt number, Lift and Drag coefficients, Strouhal

number, contours of vorticity and temperature will be drawn in the ensuing sections.

2. PHSICAL DESCRIPTION OF THE PROBLEM

The influence of a counter-rotating vortical gust is numerically examined on the forced convection heat transfer from a spinning circular cylinder and its effect on an incoming mean flow. The water is used as a working fluid at a Prandtl number of 7 (Pr = 7). The two-dimensional laminar flow is analyzed for a fixed Re of 100. Furthermore, the dimensionless spinning rate is altered from 0 to 1.5 in an equal step of 0.25 and the cylinder is rotating in a counter-clockwise direction. Fig.1-a illustrates a flow configuration of the problem that incorporates the upstream cylinder 1 and downstream cylinder 2 in a staggered arrangement as indicated by Fig.1-b.

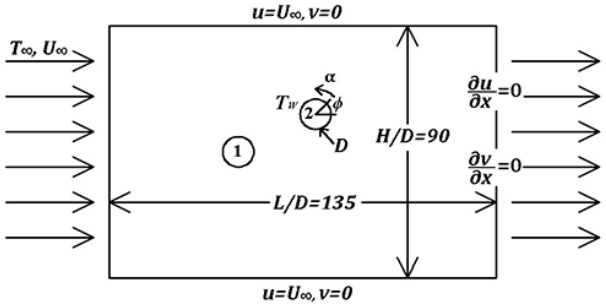

Fig. 1-a. Schematic diagram of the problem

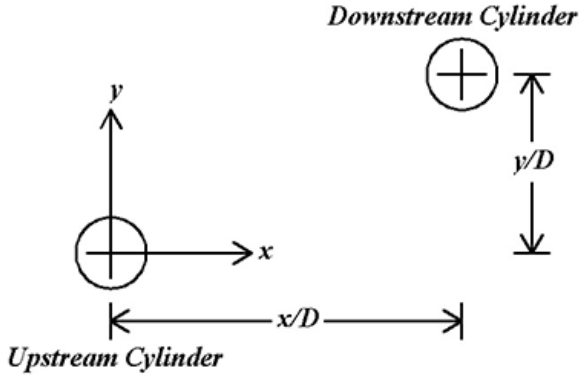

Fig. 1-b. Staggered arrangement of two circular cylinders

Both cylinders are of the same size having a unit diameter. The upstream cylinder is located at the origin while the placement of a downstream cylinder is decided by tracking a vortex center trajectory as a result of the constant rotation rate of 5, imposed to an upstream cylinder (a single cylinder case) as shown in Fig.2-a. The trajectory of a vortex center is determined by means of a Tecplot 360 software. A single clockwise rotating vortex is detached above the rotating cylinder in the flow direction, the vortex trajectory initially follows a curve path and finally becomes straight after some interval of time. The downstream cylinder center is placed at a location where a vortex just starts following a linear trajectory as presented in Fig.2-b, the vortex with essentials.

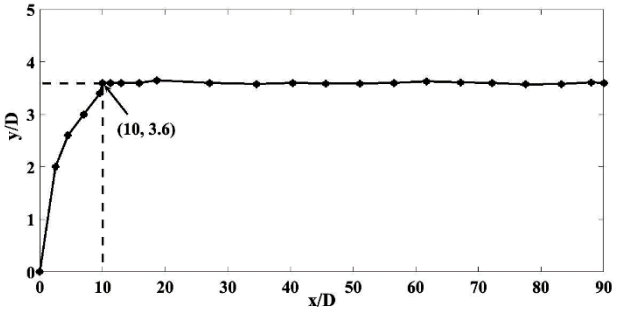

Fig. 2-a. Vortex trajectory shed from a rotating cylinder at α=5

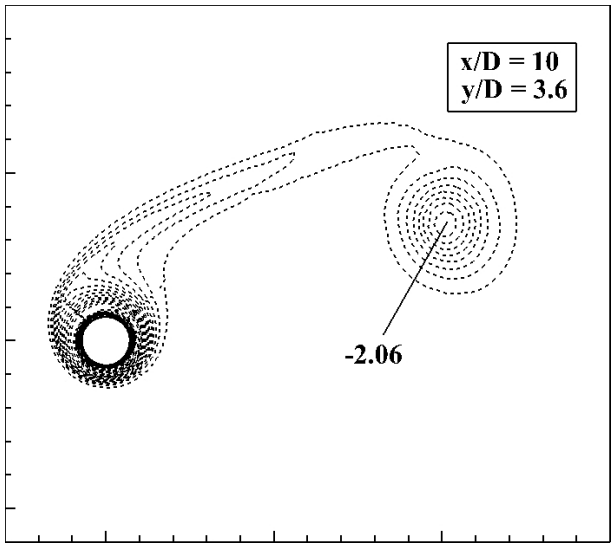

Fig. 2-b. Vortex characterization of a clockwise vortex, ($-10 \le \omega_z \le 10$)

Initially, the flow at the inlet is considered uniform with a constant mean free stream velocity (U_∞). The downstream cylinder wall is held at a fixed temperature (T_w) of 302K whereas, the mean free stream flow is sustained to a fixed temperature of 300K (T_∞). The cylinder wall acts as a source, is at a higher temperature in comparison to a mean flow that behaves like a sink and ensures the uni-directional heat transfer away from a cylinder in the fluid without changing its thermo-physical properties. The current study focuses on the downstream cylinder and the whole system behaves as a flow past a single rotating circular cylinder. The upstream cylinder acts as a vortical gust generator for all the simulation cases. While executing a solution, the mean flow interacts with

the cylinder and a regular von-Karman street develops behind the downstream cylinder. When the arrangement has attained the limit cycle oscillation pattern, a counter-rotating vortical gust pair is superimposed to the downstream cylinder. The counter-rotating vortical gust pair particulars emerge in the ensuing sections of this document.

3. GOVERNING EQUATIONS

The problem consists of a single spinning circular cylinder retained to a constant wall temperature (CWT), experienced a uniform streamlined flow imparted by a counter-rotating vortical gust pair. The transient, conservative and dimensionless form for a laminar, viscous and incompressible flow in two dimensions are the governing Continuity, Navier Stokes, and the Energy equations:

Continuity equation:

$$\frac{\partial U}{\partial X}+\frac{\partial V}{\partial Y}=0 \tag{1}$$

X- momentum equation:

$$\frac{\partial U}{\partial \tau}+\frac{\partial (UU)}{\partial X}+\frac{\partial (VU)}{\partial Y}=\frac{1}{Re}\left(\frac{\partial^2 U}{\partial X^2}+\frac{\partial^2 U}{\partial Y^2}\right)-\frac{\partial P}{\partial X} \tag{2}$$

Y-momentum equation:

$$\frac{\partial V}{\partial \tau}+\frac{\partial (UV)}{\partial X}+\frac{\partial (VV)}{\partial Y}=\frac{1}{Re}\left(\frac{\partial^2 V}{\partial X^2}+\frac{\partial^2 V}{\partial Y^2}\right)-\frac{\partial P}{\partial Y} \tag{3}$$

Thermal-energy equation:

$$\frac{\partial \theta}{\partial \tau}+\frac{\partial (U\theta)}{\partial X}+\frac{\partial (V\theta)}{\partial Y}=\frac{1}{RePr}\left(\frac{\partial^2 \theta}{\partial X^2}+\frac{\partial^2 \theta}{\partial Y^2}\right) \tag{4}$$

Here, '$U=\frac{u}{U_\infty}$' is the dimensionless stream-wise velocity and the cross-stream velocity in dimensionless form is characterized as '$V=\frac{v}{U_\infty}$'. Moreover, '$X=\frac{x}{D}$' is the dimensionless stream-wise dimension of coordinates and '$Y=\frac{y}{D}$' is the cross-stream dimension of coordinates in dimensionless form. Dimensionless time is outlined as '$\tau=\frac{tU_\infty}{D}$' and '$\theta=\frac{T-T_\infty}{T_W-T_\infty}$' is termed as the dimensionless temperature.

4. BOUNDARY CONDITIONS

The physically realistic boundary conditions are enacted to the flow configuration to solve the governing equations for the flow and temperature fields are stated as follows:

1. The uniform flow conditions are insisted at the left inlet boundary of a domain.

$$U=1,\ V=0,\ \theta=0,\ \frac{\partial P}{\partial X}=0 \tag{5}$$

2. The right boundary is subjected to a state of convective flow condition.

$$\frac{\partial \xi}{\partial \tau}+U_c\frac{\partial \xi}{\partial n}=0,\ P=0 \tag{6}$$

Where, U_c=1, ξ=U, V and θ, and n is the cylinder surface normal direction.

3. The upper and lower boundaries act as fictitious symmetric walls. An adiabatic and slip flow conditions are employed at these margins.

$$\frac{\partial U}{\partial Y}=0,\ V=0,\ \frac{\partial P}{\partial Y}=0,\ \frac{\partial \theta}{\partial Y}=0 \tag{7}$$

4. At the surface of a cylinder, a no-slip condition is imposed and cylinder surface is subjected to an isothermal temperature, resembles a Dirichlet boundary condition. The rotational boundary condition is enacted over the surface of a cylinder by rotating the cylinder wall at a given rotational speed.

$$U=-\alpha\sin\varphi,\ V=-\alpha\cos\varphi,\ \frac{\partial P}{\partial n} \tag{8}$$

$$\theta=1\ (\text{for CWT}) \tag{9}$$

The non-dimensional parameters like Reynolds number (Re), Prandtl number (Pr), Nusselt number (Nu), dimensionless rotation rate (α) and dimensionless pressure (P) are expressed as:

$$Re=\frac{U_\infty D}{\nu} \tag{10}$$

$$Pr=\frac{\mu C_P}{K} \tag{11}$$

$$Nu=\frac{hD}{K} \tag{12}$$

$$\alpha=\frac{D\omega}{2U_\infty} \tag{13}$$

$$P=\frac{P'}{\rho U_\infty^2} \tag{14}$$

5. GENERATION OF A COUNTER-ROTATING VORTICAL GUST

A counter-rotating vortical gust comprises a clockwise and anticlockwise pair, sheds in a mean free stream flow as indicated in the Fig. 3. It specifies the vortical gust configuration at three different time steps (a), (b) and (c).

The gust is generated by a suitable technique via inter-changing the boundary conditions associated with an upstream cylinder during a numerical simulation in three different steps. Initially, the upstream cylinder is considered as a velocity inlet along with the flow at the inlet, both are assumed

uniform with a free stream velocity (U_∞) and at a fixed temperature of 300K (T_∞). The velocity inlet condition at the upstream cylinder persists until the formation of typical limit cycle oscillation pattern for a downstream cylinder. After the formation of proper limit cycle oscillation behavior, the upstream cylinder is changed to a rotating wall with a constant rotation rate of 5 imposed for a small period of time. When a single clockwise rotating vortex starts growing above the cylinder (a), the wall is transformed back to velocity inlet after a small duration of time which in the present case is 4 seconds. At that moment, the shear layer that rolls around the cylinder shed down the cylinder in a counterclockwise manner (b), results in the formation of a counter-rotating vortical gust pair (c).

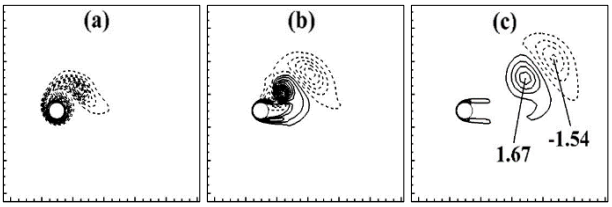

Fig. 3. Generation of a counter-rotating vortical gust pair, ($-10 \leq \omega_z \leq 10$)

6. NUMERICAL DETAILS

In the present work, a structured multi-block grid is created by means of a commercially available GAMBIT software. The grid is shown in Fig. 4 (a) along with a close-up view of a mesh around circular cylinders in (b). The grid generation is accompanied in such a way that a higher mesh distribution is kept close to a cylinder wall in order to sort out the boundary layer flow characteristics in an efficient manner.

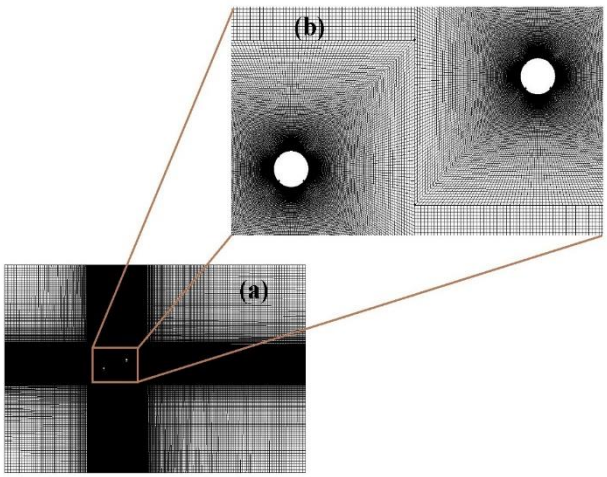

Fig. 4. Grid structure (a), Zoom-in view of grid distribution in the vicinity of cylinders (b)

The laminar, transient, two-dimensional and incompressible flow is solved by employing the pressure based segregated solvers in order to characterize the flow physics and forced convection heat transfer around a spinning circular cylinder. The governing equations can be resolved by using the semi-implicit method for pressure linked equation (SIMPLE) for suitable boundary conditions along with second order transient formulation. The convective terms are discretized via the second order upwind scheme in the momentum equations, although the diffusive expressions are discretized via central difference technique. A convergence criterion of 10^{-6} is used for the continuity, x/y components of momentum and energy equations in a consistent way. An adequate time step size of 0.001 seconds is exercised together with a maximum 50 iterations per time step to determine time step independent results for a given workout, with and without vortical gust.

7. DOMAIN AND GRID INDEPENDENCE STUDY

The domain and grid independence study play a vital role to find the simulation results free of the computational domain and the total number of nodes and cells. Mittal and Kumar [16] stated the significance of an exterior boundary position for a rotating cylinder at higher rotation rates. It means that the domain length for an outer boundary should be large enough in order to obtain the desired independent results. Different domain sizes are simulated for a stationary cylinder (α=0) and compared to the findings made by Baranyi [6] and Paramane and Sharma [20] in Table 1.

Table 1. Comparison of aerodynamic coefficients with the published literature

Domain Size	Reynolds Number (Re)	C_{Drms}	C_{Lrms}
Baranyi [6]	100	0.0064	0.228
Paramane and Sharma [20]	100	0.0062	0.227
120D X 80D (Present)	100	0.0057	0.219
135D X 90D (Present)	100	0.0061	0.226
150D X 100D (Present)	100	0.0063	0.224

The calculated aerodynamic coefficients are in good promise with the outcomes in literature. Therefore, a computational domain of L/D=135 in the longitudinal and H/D=90 in the lateral direction

together with 1,56,176 nodes and 1,55,250 quadrilateral control volumes after a grid independence study are finally used in this workout.

8. VALIDATION

The current numerical study is validated by means of the computed verdicts for some suitable parameters. Consider, for instance, the Strouhal number and average Nusselt number for a stationary single isothermal circular cylinder. The calculated values for a Strouhal number are shown in Table 2 and compared with Baranyi [6] and Shen et al. [27]. For the present work, the calculated value of a Strouhal number is 0.165 although its value comes out to be 0.163 as stated by Baranyi [6] and 0.166 as stated by Shen et al. [27]. Both values in the literature are in good agreement with the current research findings having a maximum difference of 1.2%.

Table 2. Validation of Strouhal number

Validation	Reynolds Number (Re)	Strouhal Number (St)
Baranyi [6]	100	0.163
Shen et al. [27]	100	0.166
Present	100	0.165

In contrast, the computed average Nusselt number for the present work is justified by formerly reported correlations provided by Knudsen and Katz [28] and Churchill and Bernstein [29]. Table 3 consolidates the comparison of average Nusselt number for a fixed circular cylinder. The Knudsen and Katz [28] correlation is given by equation (15):

$$\overline{Nu} = 0.683 Re^{0.466} Pr^{1/3} \quad (15)$$

Likewise, the Churchill and Bernstein [29] correlation is reproduced in (16):

$$\overline{Nu} = 0.3 + \frac{0.62 Re^{1/2} Pr^{1/3}}{\left[1+(\frac{0.4}{Pr})^{2/3}\right]^{1/4}} \left[1 + \left(\frac{Re}{282000}\right)^{5/8}\right]^{4/5} \quad (16)$$

The computed value of the average Nusselt number comes out to be 12.08 for the present numerical study. However, the Knudsen and Katz [28] correlation provides an average Nusselt number of 11.2 while a value of 11.83 is stated by the Churchill and Bernstein [29] correlation. The examined values of an average Nusselt number in the current study, match well with the aforementioned correlations together with a maximum difference of 7% is observed.

Table 3. Validation of average Nusselt number

Validation	Reynolds Number (Re)	Average Nusselt Number ($\overline{Nu}$)
(15)	100	11.2
(16)	100	11.83
Present	100	12.08

9. RESULTS AND DISCUSSION

9.1 Total lift and drag coefficient

Fig. 5-a and 5-b represent the graphical behavior of total lift and drag coefficient at specified spinning rates for the case involving no gust. The lift force increases in a monotonic manner, following the surge in the downward direction in a direct correlation to the rotation rate along with the foremost lift force pressure component. In contrast, the drag coefficient obeys the trend in a parallel mode as a consequence of a decline in the pressure drag. Both the scenarios are in good comparison with the descriptions stated by Kang et al. [11], Paramane and Sharma [20] and Sufyan et al. [24].

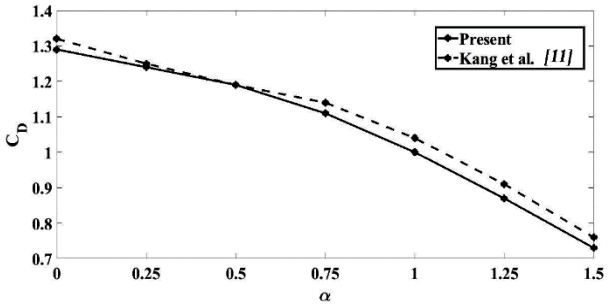

Fig. 5-a. Variation of total drag coefficient, uniform flow (without gust)

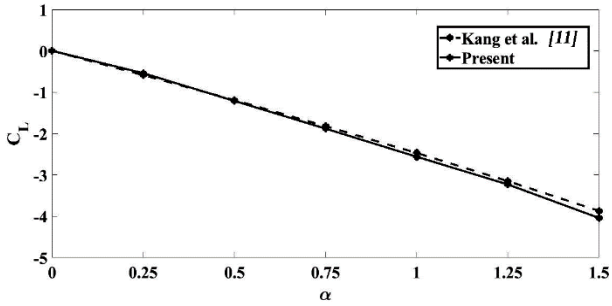

Fig. 5-b. Variation of total lift coefficient, uniform flow (without gust)

The vortical gust illustrates a significant interaction effect on the time histories of lift

coefficients, enacted to a mean free stream flow as depicted in Fig. 6.

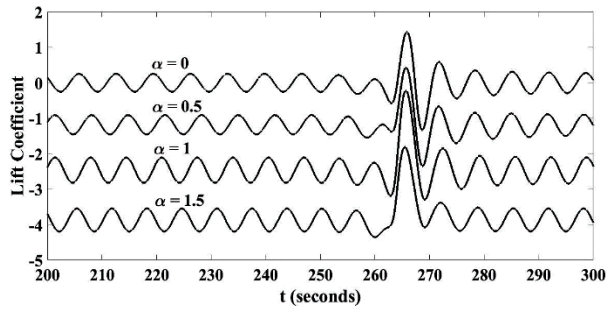

Fig. 6. Time histories of lift coefficient representing the vortical gust effect (Close up view)

Lift coefficient increases in the downward direction and the gust effects are prominent for given rotation rates. However, a transient region in the curves grows considerably with the rotation rate for progressively larger time intervals. All the lift coefficients are allowed to attain an oscillation state of a limit cycle before the commencement of vortical gust on a cylinder for all the simulations. The gust causes a sharp peak to the lift coefficient time history corresponding to its perturbation effect as a result of a decrease in instantaneous pressure distribution as presented in Fig. 7-a and 7-b, along a cylinder periphery for both without and with vortical gust circumstances.

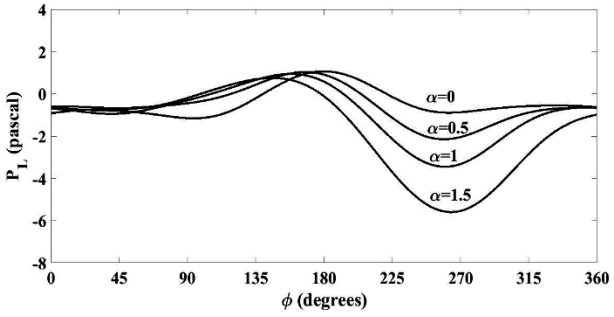

Fig. 7-a. Pressure distribution around a cylinder circumference, without gust

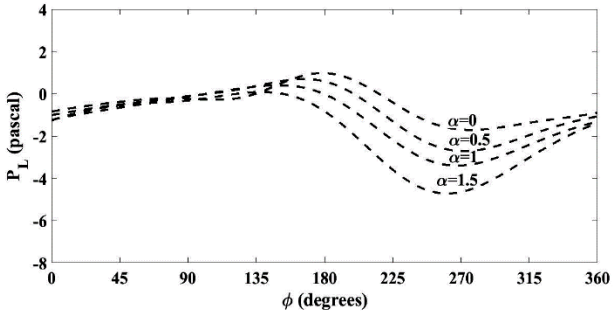

Fig. 7-b. Pressure distribution around a cylinder circumference, with gust

The enveloping layer of a static fluid around a circular cylinder becomes thicker at higher rotation rates and attributed to the decreasing trend for the instantaneous pressure phenomenon. For a fixed cylinder i.e. α=0, the sharp peak in the time history consists of upper and lower halves about a mean position. By an increase in spinning rate, the amplitude of the upper half increases and the lower half nearly diminishes as for α=1.5 shown in Fig. 6. All simulations are executed for a larger period of time so that the time histories of lift coefficients return to the limit cycle oscillation condition after the gust has passed.

9.2 Strouhal number

The average value of a dimensionless vortex shedding frequency i.e. Strouhal number (St) can be determined via carrying out a fast Fourier transform (FFT) of the lift coefficient in an appropriate way. Fig. 8 reflects the corresponding values of Strouhal number for without and with gust under the action of an oscillating lift force practiced by a rotating circular cylinder submerged in a flow stream at numerous spinning rates. The phenomenon of vortex shedding is obvious at all the selected rotation rates due to a certain value provided by a Strouhal number. The streamlined flow i.e. without gust illustrates a prevalent behavior throughout the simulation results. The determined value of a St is 0.165 for a stationary cylinder in case of uniform flow whereas, its value comes out to be 0.159 for a gust scenario and resembles a difference of 3.6%. In the same fashion, the difference blows up to about 13.3% for α=1 at higher rotation rates.

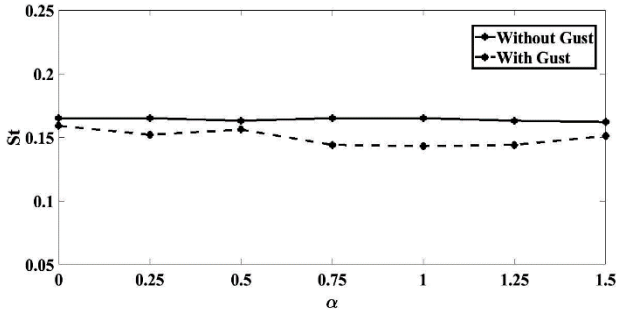

Fig. 8. Comparison of average value of Strouhal number, with and without gust

9.3 Vorticity contours

The uniform flow around a fixed cylinder yields the formation of positive and negative symmetric vortices to a cylinder wake in the form of a regular

Karman vortex street,Badr et al. [3] . Alternatively, the rotational effect imposed to a cylinder ruptures the wake evenness by enveloping the shear layer around a cylinder and a vortex detached in an asymmetric manner. The thickness of an enveloping vortex increases with the rotation rate of a cylinder alters the strength and location of a positive and negative vortex pair as suggested by Mittal and Kumar [16]. Instantaneous spanwise vorticity ($-0.4 \leq \omega_z \leq 0.4$) contours under the effect of a vortical gust are shown in Fig. 9 at four distinctive time occurrences for the designated set of rotation rates. t1; indicates the contours before the gust impingement, t2, and t3; effect of a clockwise and counterclockwise vortex pair on a circular cylinder at consistent time instances, and finally t4; flow physics behind the rotating cylinder after the gust has passed. The counter-rotating vortical gust pair is presented in the left column by uppercase alphabets **A** (negative vortex) and **B** (positive vortex) before its interaction to a cylinder.

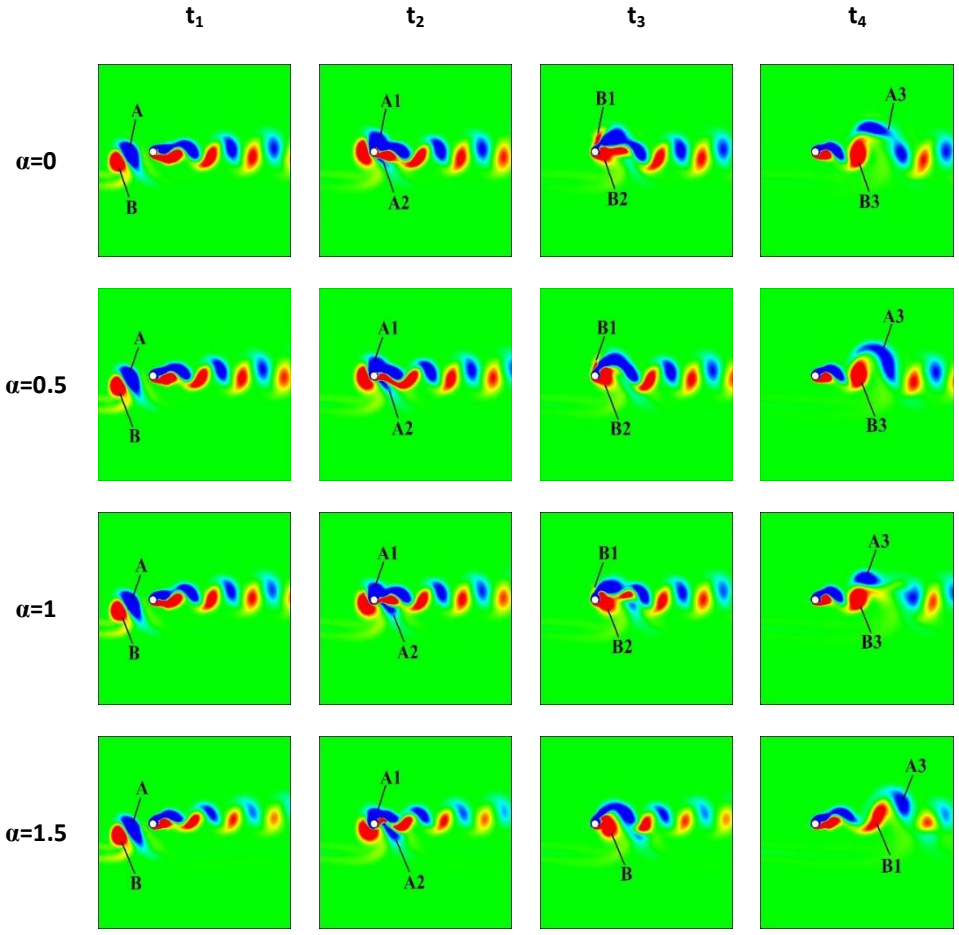

Fig. 9. Instantaneous spanwise vorticity (ω_z) contours showing the vortical gust interaction

The second and third column represents the effect of a vortical gust pair **A** and **B** on a rotating cylinder respectively. The last column displays the final formation of both vortices in the downstream wake of a circular cylinder. For all the cases, the vortex **A** splits into two vortices **A1** and **A2** after striking the cylinder. However, the vortex **B** divides into two separate vortices **B1** and **B2** up to α=1 and remains unchanged as **B** for higher rotation rates. The majority part of a vortex **A** rolls above a cylinder to combine with the clockwise formation of a vortex and at the same time, the remaining small chunk swirls below a cylinder, merges downstream and outlines a vortex **A3**. The same phenomenon is observed for the formation of a vortex **B3** until α=1 and **B1** onwards. The vortical structures detachment is clearly examined in Fig. 6 in the lift coefficient curves. As the rotation rate increases, the vortex **A2** enlarges below a cylinder periphery as indicated by a second column. In contrast, refer to the third column the size and strength of vortex **B1** dwindles for higher rotation rates and shifts towards the direction of rotation as vortex **B**. During a vortical gust interaction, the thickness of a shear layer raises and the vorticity distribution along the cylinder boundary has altered significantly. The final formation of stretched vortices in the rightmost column sheds

downstream with other vortices to a large extent and exhibits a remarkably higher strength zone under the collective effect of cylinder rotation and counter-rotating vortical gust.

9.4 Temperature contours

The rotational effect imposed by a circular cylinder on the forced convection heat transfer is greatly affected as a consequence of a thermal boundary layer formed around a cylinder periphery. As stated earlier, a cylinder surface is at a higher temperature in comparison to a surrounding fluid, promotes the heat transfer by a fixed temperature difference. The thermal shear layer chunkiness is dominant along the circumference of a cylinder, increases for the chosen rotation rates and resists the heat transfer rate to a considerable amount according to Paramane and Sharma [20]. Mahfouz and Badr [14] reported the remarkable effects on the forced convection heat transfer due to a shedding of vortical structures and the frequency of an oscillating lift force. Heat transfer rate can be enabled or disabled depending on both of these factors.

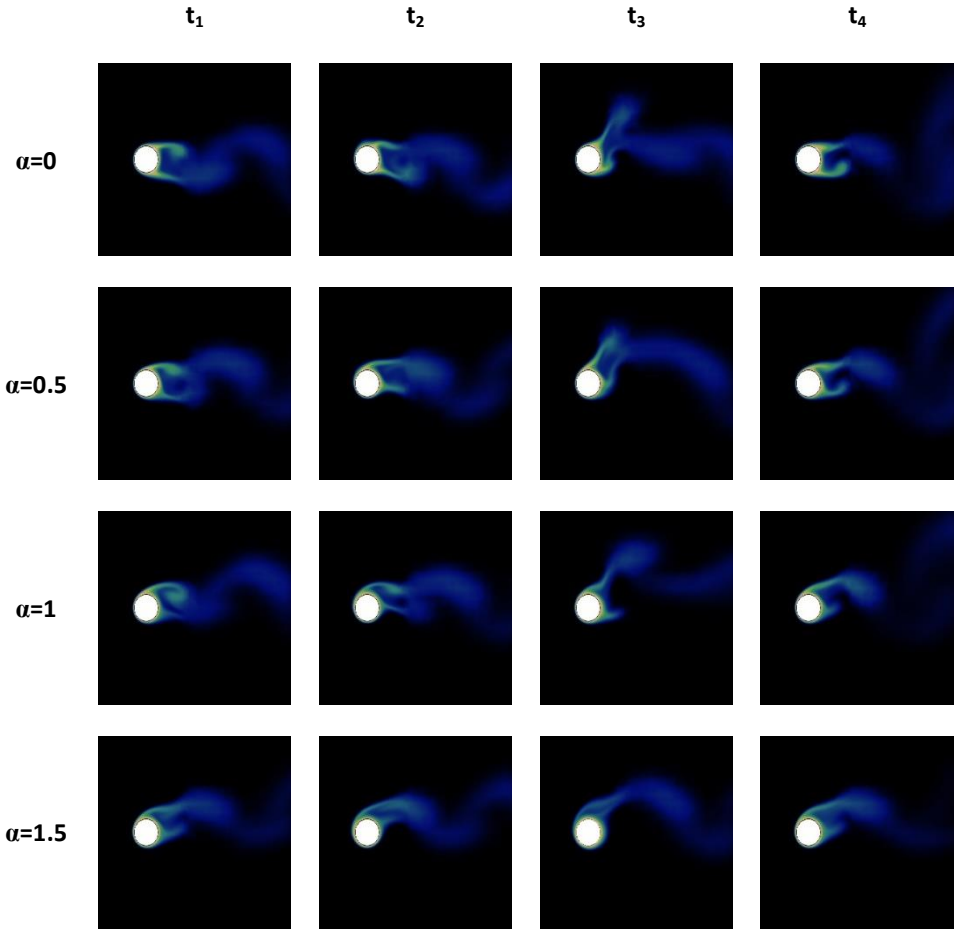

Fig. 10. Instantaneous temperature contours showing the vortical gust interaction

Instantaneous temperature contours are stated in Fig. 10 for selected rotation rates and time instances in the same mode as in the preceding section corresponding to a gust effect. The stationary cylinder causes the earlier detachment of a vortex while the rotating cylinder lags the separation of a vortical structure due to a magnus effect. The earlier detachment enhances the Strouhal number value and the convection heat transfer rate. By introducing a vortical gust to an incident flow initiates the elongation of a shear layer and modifies the vortex detaching frequency as in Ikhtiar et al. [25] and Rana et al. [26]. The shear layer stretches further with the rotation rate and the detachment period escalates that lowers the transfer of heat by convection from a rotating cylinder. The same phenomenon results in the lower values of Strouhal number as a result of a delay to a vortex shedding frequency. Moreover, the gust stretches the temperature plume remarkably for a larger period of time in comparison to a streamline flow without gust. The streamline flow promotes the quicker rate of

heat diffusion mechanism rather than vortical gust by cooling a trapped fluid inside a vortical structure as it sheds away from the rotating circular cylinder.

9.5 Local nusselt number

The local Nusselt number (Nu_L) offers an information regarding the trend of values at each point along the exterior of a cylinder. At some points, the Nusselt number is maximum while at certain points its value is minimum and the remaining values lie between them. Fig. 11-a reflects the plot of the local Nusselt number for a flow condition without gust while Fig. 11-b illustrates the behavior of a vortical gust for specified rotation rates at the surface of a cylinder. The Nu_L variation for a vortical gust illustrates a recessive trend as compared to a uniform flow. It is clearly visible that the value of a maximum Nusselt number is lower for a vortical gust case in contrast to a uniform flow around a cylinder.

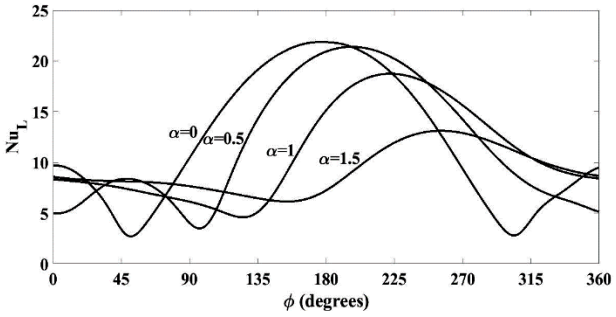

Fig. 11-a. Variation of a local Nusselt number around a cylinder circumference, without gust

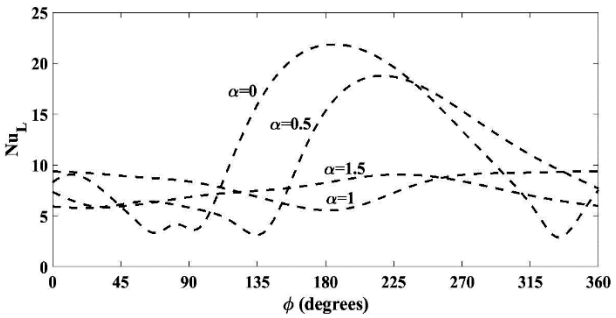

Fig. 11-b. Variation of a local Nusselt number around a cylinder circumference, with gust

In case of a fixed cylinder without gust i.e. α=0, the maximum Nusselt number appears at the front stagnation point for $\Phi=180^o$ while the least value exists at the points, $\Phi_I \approx 50^o$ and $\Phi_{II} \approx 305^o$. The local Nusselt number decreases beyond the stagnation point on both sides up to $\Phi_I \approx 50^o$ and $\Phi_{II} \approx 305^o$ then increases till reaches 0^o or 360^o. Moreover, the maximum value for the gust effect occurs at $\Phi \approx 190^o$ and the minimum one arises at three different points $\Phi_I \approx 68^o$, $\Phi_{II} \approx 95^o$ and $\Phi_{III} \approx 335^o$ respectively. In this scenario, the Nusselt number increases from $\Phi_{II} \approx 95^o$ to $\Phi \approx 190^o$ and decreases beyond it until $\Phi_{III} \approx 335^o$ and again increases up to approximately 15^o and then starts decreasing till $\Phi_I \approx 68^o$. From $\Phi_I \approx 68^o$ to $\Phi_{II} \approx 95^o$, a small jump is present having extreme value at about 82^o and declines on both sides. The variation in local Nusselt number for a spinning cylinder changes accordingly for both the flow conditions. For instance, at α=1 the maximum Nusselt number appears at $\Phi \approx 225^o$ and the minimum value exists at $\Phi_I \approx 135^o$ for uniform flow. Moreover, from gust viewpoint, the maximum Nusselt number comes out to be around $\Phi \approx 0^o$ or 360^o and the minimum one occurs at $\Phi_I \approx 180^o$ close to a front stagnation point. For both cases, the position of maximum and minimum variation in Nusselt number shifts in the spinning direction. Similarly, the local Nusselt number variation decreases at large spinning rates and the position of maximum and minimum Nusselt number changes in an appropriate way along the periphery of a circular cylinder.

9.6 Average nusselt number

The heat transfer rate from a circular cylinder depends on a relative ratio of convection and conduction phenomenon. This fact is enlightened by a non-dimensional average Nusselt number ($\overline{Nu}$) that is used to characterize the heat transfer at the surface of an object inside a fluid. For a uniform incident flow, the greater value of Re causes the $\overline{Nu}$ to increase for a convection mode of heat transfer. Furthermore, the thickness of an enveloping vortex along a periphery of a cylinder grows in a direct correspondence to a rotation rate and as a result, average Nusselt number decreases implies the heat transfer by conduction. For details see for example Mahfouz and Badr [14]. According to Paramane and Sharma [20], the fluid captured within an enveloping vortex appears as a buffer zone between the flow field and the cylinder wall. The thickness of a buffer zone increases with the spinning rate, causes the thermal resistance to enhance and decreases the heat transfer rate respectively. Ikhtiar et al. [25] and Rana et al. [26] examined the effects of a single gust impulse by using the Gaussian

distribution function on the Nusselt number behavior for the selected range of dimensionless rotation rates.

Fig. 12 depicts the comparison of $\overline{Nu}$ for without and with vortical gust for the given flow conditions. The vortical gust lowers the value of $\overline{Nu}$ for the respective rotation rates in comparison to a uniform flow. For a fixed cylinder, a decrement of 4.1% is observed whereas a maximum difference of 25.89% can be noticed at α=1.25 respectively. The vortical gust thickens the shear layer around a cylinder in a more typical manner in contrast to a uniform flow. This enhanced thickness increases with the rotation rate due to further stretching of a shear layer in the downstream wake as observed in the temperature contours. As a result, the conduction mode is dominant over a convection mode of heat transfer yielding an inclusive decrease to an average Nusselt number.

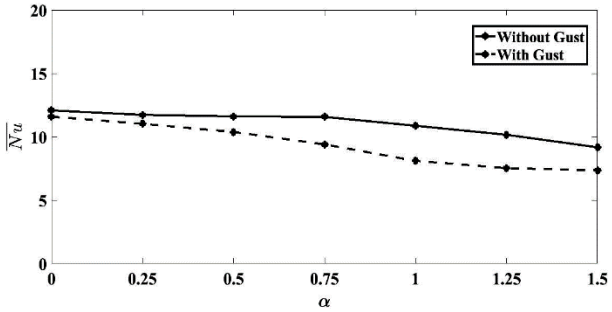

Fig. 12. Comparison of an average Nusselt number, with and without gust

10. CONCLUSION

The following conclusions can be extracted for this research on the behalf of above results analysis.

1. The lift coefficient time histories characterize the interesting facts under the action of a vortical gust in the form of sharp kinks. At low rotation rates, the gust effect comprises of both upper and lower halves in a time history. The amplitude of an upper half increases whereas the lower half diminishes in direct correspondence at higher rotation rate due to a net effect insisted by a vortical gust pair.

2. The shear layer enlarges by a vortical gust pair in a direct correspondence to a rotation rate. Enlargement in the shear layer causes the late detachment of a vortex and thus affects the shedding frequency. This leads to a lesser value of Strouhal number as compared to a streamline flow involving no gust.

3. The thickness of a temperature plume is sensitive to a vortical gust. Gust causes the thickness to increase further and resists the heat transfer rate for a rotating cylinder. At higher rotation rates, heat transfer by conduction is more prominent rather than convection.

4. The position of maximum and minimum local Nusselt number varies accordingly along the circumference of a rotating cylinder for both cases i.e. without and with gust. The gust reduces the value of an average Nusselt number with a minimum and maximum decrement of 4.1% and 25.89% was detected.

ACKNOWLEDGEMENT

The study was supported and funded by Mechanical Engineering Department, University of Engineering and Technology Taxila, Pakistan, which is gratefully acknowledged.

REFERENCES

[1] B. Fornberg, A numerical study of steady viscous flow past a circular cylinder. *Journal of Fluid Mechanics*, 98(4), 1980: 819-855. https://doi.org/10.1017/S0022112080000419

[2] C. Lange, F. Durst, M. Breuer, Momentum and heat transfer from cylinders in laminar crossflow at 10− 4⩽ Re⩽ 200. *International Journal of Heat and Mass Transfer*, 41(22), 1998: 3409-3430. https://doi.org/10.1016/S0017-9310(98)00077-5

[3] H. Badr, S. Dennis, P. Young, Steady and unsteady flow past a rotating circular cylinder at low Reynolds numbers. *Computers & Fluids*, 17(4), 1989: 579-609. https://doi.org/10.1016/0045-7930(89)90030-3

[4] D. Barkley, R.D. Henderson, Three-dimensional Floquet stability analysis of the wake of a circular cylinder. *Journal of Fluid Mechanics*, 3221996: 215-241. https://doi.org/10.1017/S0022112096002777

[5] C.H. Williamson, Vortex dynamics in the cylinder wake. *Annual review of fluid mechanics*, 28(1), 1996: 477-539. https://doi.org/10.1146/annurev.fl.28.010196.002401

[6] L. Baranyi, Computation of unsteady momentum and heat transfer from a fixed circular cylinder in laminar flow. *Journal of computational and applied Mechanics*, 4(1), 2003: 13-25.

[7] A. Roshko, Experiments on the flow past a circular cylinder at very high Reynolds

number. *Journal of Fluid Mechanics*, 10(3), 1961: 345-356.
https://doi.org/10.1017/S0022112061000950

[8] M. Coutanceau, C. Menard, Influence of rotation on the near-wake development behind an impulsively started circular cylinder. *Journal of Fluid Mechanics*, 158, 1985: 399-446.
https://doi.org/10.1017/S0022112085002713

[9] D. Ingham, T. Tang, Numerical investigation into the steady flow past a rotating circular cylinder at low and intermediate Reynolds numbers. *Journal of Computational Physics*, 84, 1989: 256-257.
https://doi.org/10.1016/0021-9991(90)90227-R

[10] H. Badr, S. Dennis, Time-dependent viscous flow past an impulsively started rotating and translating circular cylinder. *Journal of Fluid Mechanics*, 158, 1985: 447-488.
https://doi.org/10.1017/S0022112085002725

[11] S. Kang, H. Choi, S. Lee, Laminar flow past a rotating circular cylinder. *Physics of Fluids*, 11(11), 1999: 3312-3321.
https://doi.org/10.1063/1.870190

[12] C. Hieber, B. Gebhart, Low Reynolds number heat transfer from a circular cylinder. *Journal of Fluid Mechanics*, 32(1), 1968: 21-28.
https://doi.org/10.1017/S002211206800056X

[13] A. A. Kendoush, An approximate solution of the convective heat transfer from an isothermal rotating cylinder. *International Journal of Heat and Fluid Flow*, 17(4), 1996: 439-441.
https://doi.org/10.1016/0142-727X(95)00002-8

[14] F. Mahfouz, H. Badr, Forced convection from a rotationally oscillating cylinder placed in a uniform stream. *International journal of heat and mass transfer*, 43(17), 2000: 3093-3104.
https://doi.org/10.1016/S0017-9310(99)00326-9

[15] D. Stojković, M. Breuer, F. Durst, Effect of high rotation rates on the laminar flow around a circular cylinder. *Physics of fluids*, 14(9), 2002: 3160-3178.
https://doi.org/10.1063/1.1492811

[16] S. Mittal, B. Kumar, Flow past a rotating cylinder. *Journal of fluid mechanics*, 476, 2003: 303-334.
https://doi.org/10.1017/S0022112002002938

[17] S. Sanitjai, R. Goldstein, Forced convection heat transfer from a circular cylinder in crossflow to air and liquids. *International journal of heat and mass transfer*, 47(22), 2004: 4795-4805.
https://doi.org/10.1016/j.ijheatmasstransfer.2004.05.012

[18] A. Ishak, R. Nazar, I. Pop, Unsteady mixed convection boundary layer flow due to a stretching vertical surface. *Arabian Journal for Science & Engineering (Springer Science & Business Media BV)*, 31, 2006: 165-182.

[19] R.P. Bharti, R. Chhabra, V. Eswaran, A numerical study of the steady forced convection heat transfer from an unconfined circular cylinder. *Heat and mass transfer*, 43(7), 2007: 639-648.
https://doi.org/10.1007/s00231-006-0155-1

[20] S.B. Paramane, A. Sharma, Numerical investigation of heat and fluid flow across a rotating circular cylinder maintained at constant temperature in 2-D laminar flow regime. *International Journal of Heat and Mass Transfer*, 52(13-14), 2009: 3205-3216.
https://doi.org/10.1016/j.ijheatmasstransfer.2008.12.031

[21] V.K. Patnana, R.P. Bharti, R.P. Chhabra, Two-dimensional unsteady forced convection heat transfer in power-law fluids from a cylinder. *International Journal of Heat and Mass Transfer*, 53(19-20), 2010: 4152-4167.
https://doi.org/10.1016/j.ijheatmasstransfer.2010.05.038

[22] S. Sarkar, A. Dalal, G. Biswas, Unsteady wake dynamics and heat transfer in forced and mixed convection past a circular cylinder in cross flow for high Prandtl numbers. *International Journal of Heat and Mass Transfer*, 54(15-16), 2011: 3536-3551.
https://doi.org/10.1016/j.ijheatmasstransfer.2011.03.032

[23] V. Sharma, K.A. Dhiman, Heat transfer from a rotating circular cylinder in the steady regime: Effects of Prandtl number. *Thermal Science*, 16(1), 2012: 79-91.
http://dx.doi.org/10.2298/TSCI100914057S

[24] M. Sufyan, S. Manzoor, N.A. Sheikh, Heat transfer suppression in flow around a rotating circular cylinder at high Prandtl number. *Arabian Journal for Science and Engineering*, 39(11), 2014: 8051-8063.
https://doi.org/10.1007/s13369-014-1337-7

[25] U. Ikhtiar, S. Manzoor, N.A. Sheikh, M. Ali, Free stream flow and forced convection heat transfer around a rotating circular cylinder subjected to a single gust impulse. *International Journal of Heat and Mass Transfer*, 99, 2016: 851-861.
https://doi.org/10.1016/j.ijheatmasstransfer.2016.04.045

[26] K. Rana, , S. Manzoor, N.A. Sheikh, M. Ali, H.M. Ali, Gust response of a rotating circular cylinder in the vortex suppression regime. *International Journal of Heat and Mass Transfer*, 115, 2017: 763-776.
https://doi.org/10.1016/j.ijheatmasstransfer.2017.08.059

[27] L. Shen, E.-S. Chan, P. Lin, Calculation of hydrodynamic forces acting on a submerged moving object using immersed boundary method. *Computers & Fluids*, 38(3), 2009: 691-702. https://doi.org/10.1016/j.compfluid.2008.07.002

[28] J.G. Knudsen, D.L. Katz, Fluid dynamics and heat transfer, McGraw-Hill, New York, 1958.

[29] S. Churchill, M. Bernstein, A correlating equation for forced convection from gases and liquids to a circular cylinder in crossflow. *Journal of Heat Transfer*, 99(2), 1977: 300-306. http://dx.doi.org/10.1115/1.3450685